



Finite element analysis of two basic composites

Nielsen, Lauge Fuglsang

Publication date:
2004

Document Version
Publisher's PDF, also known as Version of record

[Link back to DTU Orbit](#)

Citation (APA):
Nielsen, L. F. (2004). Finite element analysis of two basic composites. (BYG Rapport; No. R-089).

DTU Library

Technical Information Center of Denmark

General rights

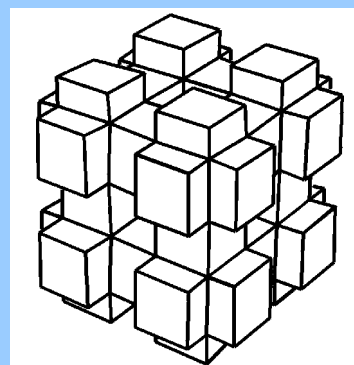
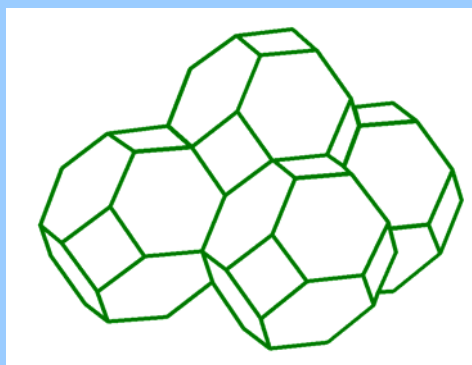
Copyright and moral rights for the publications made accessible in the public portal are retained by the authors and/or other copyright owners and it is a condition of accessing publications that users recognise and abide by the legal requirements associated with these rights.

- Users may download and print one copy of any publication from the public portal for the purpose of private study or research.
- You may not further distribute the material or use it for any profit-making activity or commercial gain
- You may freely distribute the URL identifying the publication in the public portal

If you believe that this document breaches copyright please contact us providing details, and we will remove access to the work immediately and investigate your claim.

Finite Element Analysis of two basic Composites

Lauge Fuglsang Nielsen



DANMARKS
TEKNISKE
UNIVERSITET



Documentation report
BYG•DTU R-089
June 2004
ISSN 1601-2917
ISBN 87-7877-153-6

Finite Element Analysis of two basic Composites

Lauge Fuglsang Nielsen

Preface and readers guidance

A composite theory has been presented in (1,2) on stiffness prediction of isotropic composites. The composite geometries are thought of as stages in a process of one phase transforming its geometry from spherical shapes to anti-spherical shapes (shells). In a complementary way the other phase transforms from shells to spheres.

In other words, the general composite geometry considered is the one outlined in Figure c: Namely, a transition geometry between the so-called CSA geometries (Composite Spheres Assemblage) shown in Figures a and b.

A number of numerical evaluations have been made in order to justify this geometrical concept which is the basis of the composite theory presented in (1,2): *A theory by which composite stiffness and internal stresses can be predicted for any composite geometry.*

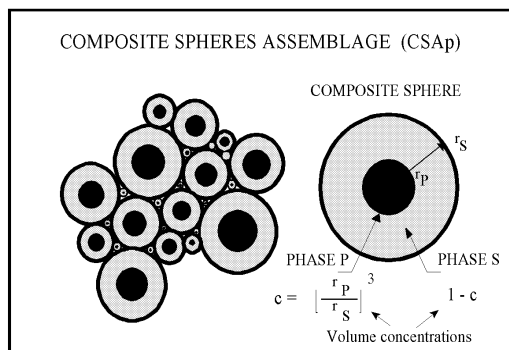


Figure a. A so-called Composite Spheres Assemblage: Here spheres of phase P embedded in a continuous phase S.

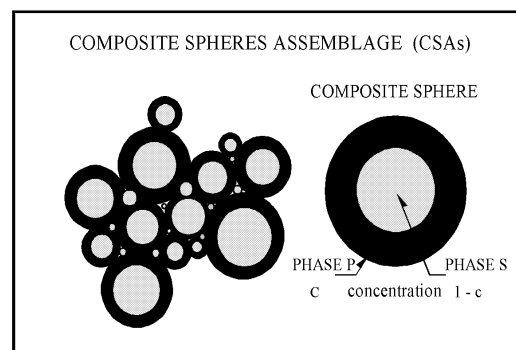


Figure b. A so-called Composite Spheres Assemblage: Here spheres of phase S embedded in a continuous phase P.

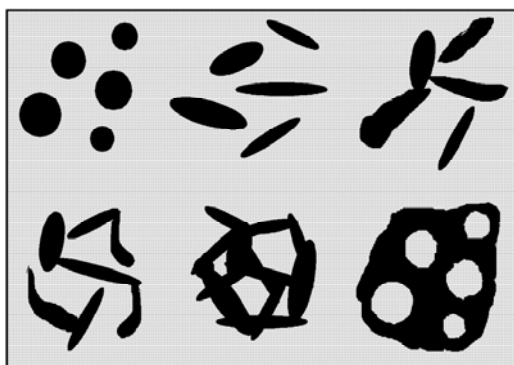


Figure c. Potential composite geometries going from CSA_p to CSA_s . Black and gray areas denote Phase P and phase S respectively.

The present report is the complete documentation for a finite element analysis made on three basic composites (parts have previously been reported in (1,3)). The composites considered are the following (with four-letter definitions explained in Figure d):

- DC-DC composites: Compact (Discrete) phase P particles in a continuous phase S matrix ("*Particulate composites*").
- CC-CC composites: Interconnected compact phase P particles in a continuous phase S matrix ("*pearls on a string composites*").
- CC-CC composites: Three-dimensional grids of one phase in complementary grids of the other phase ("*Grid composites*").
- A special analysis of the influence of *defective phase-contacts* on composite stiffness is made as part of the analysis of particulate composites.

The text of the report is self-contained in the sense that principles and symbols used are explained in Appendix A at the end of the report. The reader is kindly asked to 'go through' this appendix before she reads the main section.

It is all over understood that concentration c means volume fraction of phase P as defined in the following expression where volumes are indicated by V . Phase S concentration is then $1 - c$.

$$c = \frac{V_P}{V_P + V_S} \quad (\text{phase P}) ; \quad 1 - c = \frac{V_S}{V_P + V_S} \quad (\text{phase S})$$

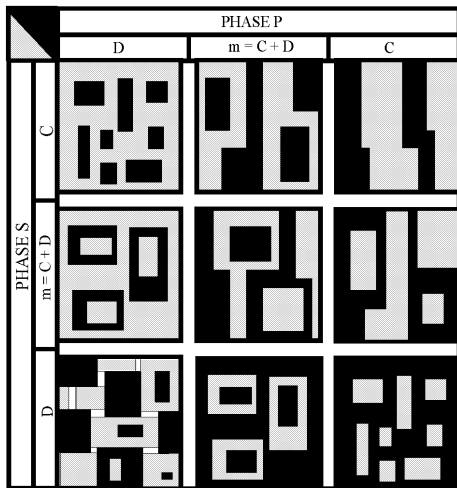


Figure d. Stylized phase geometries in two-phase materials. C , D and $m (= C + D)$ denote continuous geometry, discrete geometry, and mixed geometry respectively. A DC-CD composite has a DC-geometry at a phase P volume concentration of $c \approx 0$ and a CD-geometry at $c \approx 1$.

Remark: The nature of being a documentation report is emphasized. Only raw-data – and raw-data treated with well-justified averaging procedures are presented. Any application and graphical presentations of the data must be studied in (1,2,3) and other publications referred to in these references.

The overall accuracy of the FEM-analysis made is evaluated in a special section of the report.

Contents

PREFACE AND READERS GUIDANCE	1
CONTENTS	3
INTRODUCTION	5
2. PRELIMINARIES	5
2.1 Cubical elasticity	5
2.2 Isotropy	6
3. ANALYSIS OF PARTICULATE COMPOSITE (DC-DC).....	6
3.1 Model	6
Test volume and FEM-division.....	6
FEM-setup.....	8
FEM-results.....	8
4. ANALYSIS OF DEFECTIVE PARTICULATE COMPOSITE.....	11
4.1 FEM-setup and results	11
Defects as cracks	11
A cracked homogeneous material	12
5. PEARLS ON A STRING COMPOSITE (CC-CC)	14
5.1 FEM-setup and results	14
6. GRID COMPOSITE (CC-CC).....	16
6.1 Model	16
6.2 Test volume and FEM-division.....	16
FEM-setup.....	17
FEM-results.....	17
7. ON THE ACCURACY OF FEM-ANALYSIS	20
7.1 False data.....	21
APPENDIX A - ELASTICITY	22
A.1 Isotropy	22
A.1.1 Composite aspects	22
A.1.2 Stress-strain	22
A.2 Cubic elasticity	23
A.2.1 Poly-cubic elasticity	23
A.2.2 Composite aspects	24
LITERATURE	25

Introduction

As previously mentioned, parts of the FEM-analysis considered has previously been reported in (1,3). The complete analysis, however, is presented in this report together with references made to the original research reports (4,5,6,7,8,9,10). The FEM-method used is STRUDL (11).

2. Preliminaries

Composite models used in the FEM-analysis presented are models that can be made by a tight stacking of equally sized congruent *composite elements*. A number of composite elements form so-called *basic-cells* (such as cubic cells), which repeat themselves into a macro model of the material considered. A *test volume* for FEM-analysis is volume large enough to represent the macro model with respect to specific material property considered in analysis. Test volumes can be small as they are in the present study (smaller than the volume of a basic cell) when they are carefully selected with respect to loading and materials symmetry.

2.1 Cubical elasticity

The material models presented have cubic basic cells which means that cubical elasticity (E_C , ν_C , and G_C) of the macro model (material model) can be determined by the following "theoretical FEM-experiments", see Appendix A, cubical elasticity. Only two experiments are needed. The cubic Young's modulus and the cubic Poisson's ratio are obtained from the "axial experiment" explained in Equation 1. The cubic shear modulus is obtained from the "shear experiment" explained in Equation 2. The results of the axial experiment can be checked by the "control experiment" explained in Equation 3 from which the (E_C, ν_C)-dependent cubic bulk modulus K_C can be obtained.

AXIAL EXPERIMENT	
Conditions :	$\epsilon_x = \epsilon_y = \epsilon_{xy} = \epsilon_{xz} = \epsilon_{yz} = 0$
Load :	$\epsilon_z = 10^{-4}$
Responses :	$\sigma_x (= \sigma_y)$
Results :	$E_C = \frac{\sigma_z^2 - 2\sigma_x^2 + \sigma_x\sigma_z}{\epsilon_z(\sigma_x + \sigma_z)} ; \quad \nu_C = \frac{\sigma_x}{\sigma_x + \sigma_z}$

SHEAR EXPERIMENT	
Conditions :	$\epsilon_x = \epsilon_y = \epsilon_z = \epsilon_{xz} = \epsilon_{yz} = 0$
Load :	$\epsilon_{xy} = 10^{-4}$
Responses :	σ_{xy}
Results :	$G_C = \frac{\sigma_{xy}}{2\epsilon_{xy}}$

Control experiment	
Conditions :	$\epsilon_{xz} = \epsilon_{xy} = \epsilon_{yz} = 0$
Load :	$\epsilon_x = \epsilon_y = \epsilon_z = 10^{-4}$
Responses :	$\sigma_z (= \sigma_x = \sigma_y)$
Results :	$K_C = \frac{\sigma_z}{3\epsilon_z} \left(= \frac{E_C}{3(1 - 2\nu_C)} \right)$

2.2 Isotropy

Isotropic material models can be thought of as isotropic mixtures of parts from cubic model sources. These sources may have different sizes of composite elements which allows for size gradation in the total composite. Isotropic stiffness is converted from cubic stiffness by Equations 4 and 5 reproduced from Appendix A, poly-cubic elasticity. The isotropic bulk modulus is calculated exact. The isotropic shear modulus is given by upper and lower g-bound solutions. In the present analysis the bounds are sufficiently close to justify a simple mean value approximation.

$$\left(\frac{1}{G_C} + \frac{2}{5} \left(\frac{2(1+\nu_C)}{E_C} - \frac{1}{G_C} \right) \right)^{-1} \leq G \leq G_C + \frac{2}{5} \left(\frac{E_C}{2(1+\nu_C)} - G_C \right) \quad (4)$$

$$K = K_C = \frac{E_C}{3(1-2\nu_C)} \quad (5)$$

3. Analysis of particulate composite (DC-DC)

3.1 Model

The so-called TROC-composite outlined in Figures 1 and 2 is considered. It is a tight composition of identical composite elements each of which has the shape of a TRuncated OCTahedron with edges of equal lengths. The composite element is reinforced by a centrally placed particle the shape and orientation of which are similar to the composite element itself.

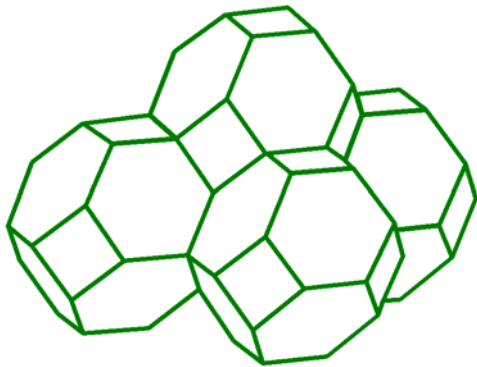


Figure 1. Stacked TROC-elements. Distance between square faces of element is 1.

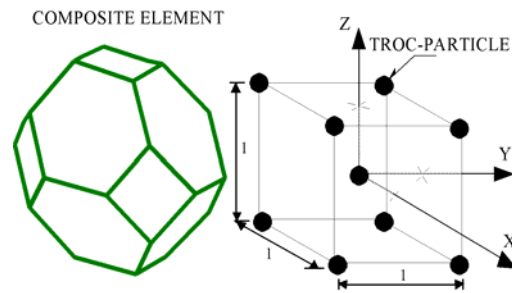


Figure 2. TROC-composite: Composite element and basic cell. Length unit 1 is height of composite element.

Test volume and FEM-division

Due to symmetry and antimetry with respect to both materials model and the FEM-setup, subsequently explained, a test volume of only 1/16 of the basic cell is used in the stiffness analysis of TROC-composites. The test volume and basic cell are shown in Figure 3. Another illustration of the test volume is shown in Figure 4 with coordinate system and symbols introduced which define the FEM-division subsequently used.

With θ and θ' as points of affinity the test volume is divided into 2 times 13 layers affine to the surfaces $C'B'EABDD'$ and $CBEA'B'D'D$ respectively, see Figure 5. Thickness of layers can be chosen arbitrarily. By taking the factors of affinity as independent variables this feature gives us the possibility of choosing an arbitrary volume concentration of particles (defined as the area inside a layer).

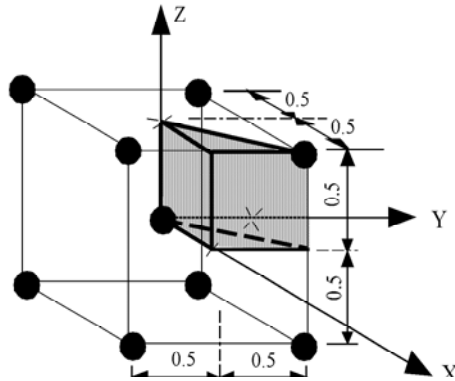


Figure 3. Basic cell and test volume for FEM-analysis of TROC-composite

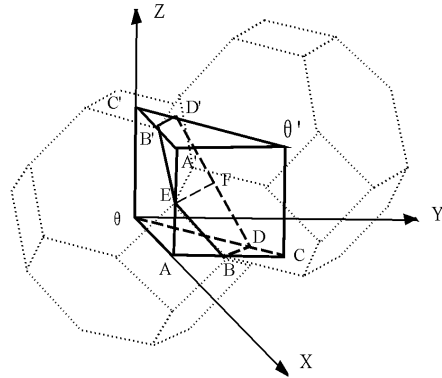


Figure 4. Test volume for FEM-analysis of TROC-composite.

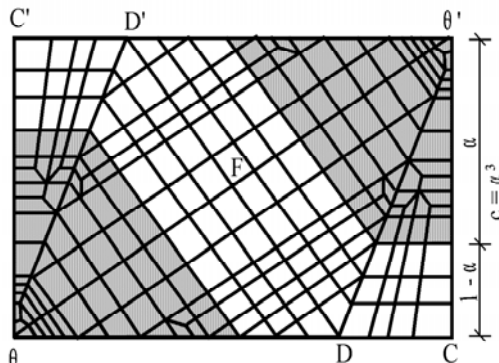


Figure 5. FEM-division of test volume in $X = Y$. Shaded areas are TROC-particles. Arbitrarily chosen phase P concentration c . (As illustrated $c \approx 0.34$).

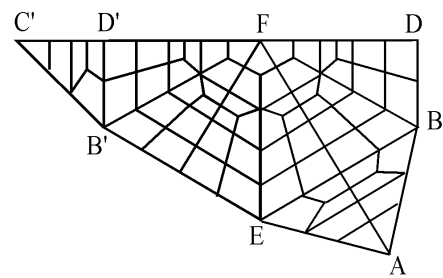


Figure 6. Principle of FEM-division of test volume. Unfolded surface of TROC-element.

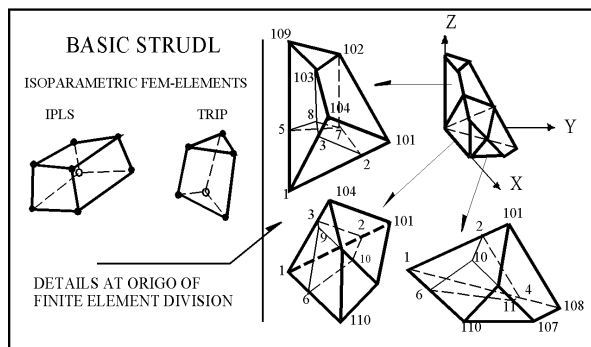


Figure 7. FEM-elements used and some combinations.

Every layer is then subdivided into finite elements as shown in Figure 6. The elements used are isoparametric and of the types IPLS and TRIP defined in (11), see Figure D7. The total amount of finite elements in the basis element is 738 with 948 sets of joint coordinates. The supporting joints in planes $AA'\theta'C$ and $A'C'\theta'$ are modified by infinitely stiff bars to pick up reaction forces on the test volume. The

version of the finite element program applied, STRUDL (11), is unable to give reactions directly from finite element joints.

A detailed description of the finite element division is given in (4). This reference also describes a program which is developed to generate automatically the 1255 sets of joint coordinates needed when changing the particle concentration (factors of affinity).

FEM-setup

The following set-ups are designed to execute the experiments outlined in Equations 1-3. The average strain is joint movement divided by associated length (0.5) of test volume, see Figure 3. The average stress is sum of bar forces divided by associated surface area of test volume.

AXIAL EXPERIMENT

Conditions: All joints in faces of test volume are smoothly supported against infinitely stiff parallel walls.

Load: Joints in face $A\theta C$ are moved $0.5 \cdot 10^{-4}$ in Z-direction.

Response: Sum of Z-forces picked up from bars in face $A'C'\theta'$

SHEAR EXPERIMENT

Conditions: All joints in faces of test volume except $A\theta C'A'$ and $AA'\theta'C$ are smoothly supported against infinitely stiff parallel walls. The joints in face $A\theta C'A'$ can move freely only in Y-direction. Joints in $AA'\theta'C$ can move freely only in X-direction.

Load: All joints in face $A\theta C'A'$ are moved $0.5 \cdot 10^{-4}$ in X-direction.

Response: Sum of Y-forces picked up from bars in face $AA'\theta'C$

CONTROL EXPERIMENT (spot checks only)

Conditions: As in axial experiment.

Load: Joints in face $A\theta C$ are moved $0.5 \cdot 10^{-4}$ in Z-direction. Face $AA'\theta'C$ is moved $-0.5 \cdot 10^{-4}$ in X-direction.

Response: Sum of Z-forces picked up from bars in face $A'C'\theta'$

FEM-results

A number of FEM-experiments have been made varying the stiffness parameters and the volume concentrations (see Figure 5) of the TROC-model. The variables are summarized as follows:

Variables: $c = 0.22 - 0.86$, $v_s = 0 - 0.4$, $v_p = 0 - 0.4$, $n = 0 - 10^5$

The raw data obtained from the axial experiment (σ_X, σ_Y) and the shear experiment (σ_{XY}) are presented in Table 1. Cubic stiffness parameters derived from these data by Equations 2 and 3 are presented in Table 2. Isotropic stiffness parameters derived from Equations 4 and 5 are presented in Table 3.

n	c	ES	vS	vS	σ_x	σ_z	σ_{xy}
.0	.216	8.e5	.2	.2	14.71278	55.06929	43.23578
.0	.343	8.e5	.2	.2	11.68733	40.53782	32.33229
.0	.512	8.e5	.2	.2	8.29173	25.76719	20.28353
.0	.729	8.e5	.0	.2	2.19976	11.43127	10.40773
.0	.729	8.e5	.2	.2	4.35933	12.12563	8.88100
.0	.729	8.e5	.4	.2	7.97351	14.75839	7.93490
.0	.8574	8.e5	.0	.2	1.22059	5.55475	4.76655
.0	.8574	8.e5	.2	.2	2.21903	5.84648	4.02942
.0	.8574	8.e5	.4	.2	3.78670	6.93173	3.55923
1/14	.729	2.e5	.4	.0	2.02856	5.30578	3.56397
.1	.512	2.e5	.2	.2	2.46370	8.63511	6.71724
1/3	.512	2.e5	.2	.2	3.36936	13.00879	9.92820
1/3	.729	2.e5	.2	.2	2.64806	10.24968	7.79571
1.	.5	6.e5	.2	.2	16.68391	66.73593	50.05188
3.	.216	2.e5	.2	.2	6.95928	27.63501	20.93380
3.	.512	2.e5	.2	.2	9.49556	37.53126	28.90596
3.	.729	2.e5	.2	.2	12.03125	47.74705	36.73804
10.	.512	2.e5	.2	.2	13.90655	54.83788	44.99459
10.	.729	2.e5	.2	.2	22.24486	89.02735	73.71604
35/3	.729	2.e5	.2	.4	39.03639	105.92799	73.82064
100.	.512	2.e5	.2	.2	17.21308	68.72851	60.51260
100.	.729	2.e5	.2	.2	33.13180	138.70803	128.49007
1.e5	.729	2.e5	.0	.2	21.06033	145.07626	144.18834
1.e5	.729	2.e5	.2	.2	35.15577	147.93230	140.50922
1.e5	.729	2.e5	.4	.2	107.13340	237.20075	197.75796

Table 1. Reaction stresses (kp/cm^2) in experiments on plain TROC-composite. Axial σ_x and σ_y . Shear: σ_{xy} .

n	c	v_s	v_p	E_{CUB}/E_s	v_{CUB}	G_{CUB}/G_s
.00000	21600	.20000	.20000	.61082	.21084	.64854
.00000	34300	.20000	.20000	.44134	.22379	.48498
.00000	.51200	.20000	.20000	.27162	.24345	.30425
.00000	.72900	.00000	.20000	.13402	.16138	.13010
.00000	.72900	.20000	.20000	.12275	.26444	.13321
.00000	.72900	.40000	.20000	.11456	.35076	.13886
.00000	.85740	.00000	.20000	.06394	.18015	.05958
.00000	.85740	.20000	.20000	.05782	.27513	.06044
.00000	.85740	.40000	.20000	.05320	.35329	.06229
.07143	.72900	.40000	.00000	.20918	.27658	.24948
.10000	.51200	.20000	.20000	.37707	.22198	.40303
.33330	.51200	.20000	.20000	.58112	.20572	.59569
.33330	.72900	.20000	.20000	.45812	.20531	.46774
1.00000	50000	.20000	.20000	1.00104	.20000	1.00104
3.00000	21600	.20000	.20000	1.24175	.20117	1.25603
3.00000	.51200	.20000	.20000	1.68483	.20192	1.73436
3.00000	.72900	.20000	.20000	2.14521	.20126	2.20428
10.00000	.51200	.20000	.20000	2.46057	.20229	2.69968
10.00000	.72900	.20000	.20000	4.00666	.19991	4.42296
11.66700	.72900	.20000	.40000	4.24522	.26928	4.42924
100.00000	.51200	.20000	.20000	3.09167	.20029	3.63076
100.00000	.72900	.20000	.20000	6.29660	.19281	7.70940
100000.00000	.72900	.00000	.20000	6.98684	.12677	7.20942
100000.00000	.72900	.20000	.20000	6.72157	.19202	8.43055
100000.00000	.72900	.40000	.20000	8.52677	.31113	13.84306

Table 2. Cubic stiffness of plain TROC-composite.

FEM analysis of two basic composites

n	c	v_s	v_p	G/G_s	K/K_s	E/E_s	v
.00000	.21600	.20000	.20000	.63054	.63371	.63117	.20120
				.63126	-	.63175	.20093
.00000	.34300	.20000	.20000	.46265	.47934	.46590	.20842
				.46409		.46707	.20768
.00000	.51200	.20000	.20000	.28588	.31763	.29171	.22448
				.28740		.29298	.22328
.00000	.72900	.00000	.20000	.12379	.19788	.14144	.14262
				.12422		.14181	.14168
.00000	.72900	.20000	.20000	.12598	.15633	.13107	.24848
				.12653		.13154	.24757
.00000	.72900	.40000	.20000	.13004	.07676	.12429	.33808
				.13081		.12495	.33723
.00000	.85740	.00000	.20000	.05730	.09995	.06680	.16584
				.05742		.06691	.16258
.00000	.85740	.20000	.20000	.05788	.07713	.06092	.26307
				.05803		.06105	.26254
.00000	.85740	.40000	.20000	.05917	.03626	.05678	.34343
				.05939		.05697	.34291
.07143	.72900	.40000	.00000	.24104	.09363	.21814	.26701
				.24145		.21846	.26668
.10000	.51200	.20000	.20000	.38926	.40688	.39266	.21048
				.38993		.39321	.21008
.33330	.51200	.20000	.20000	.58864	.59243	.58939	.20154
				.58876		.58949	.20149
.33330	.72900	.20000	.20000	.46301	.46637	.46368	.20173
				.46308		.46374	.20170
1.00000	.50000	.20000	.20000	1.00104	1.00104	1.00104	.20000
				1.00104		1.00104	.20000
3.00000	.21600	.20000	.20000	1.24979	1.24661	1.24915	.19939
				1.24983		1.24919	.19938
3.00000	.51200	.20000	.20000	1.71309	1.69567	1.70958	.19754
				1.71347		1.70988	.19749
3.00000	.72900	.20000	.20000	2.17933	2.15429	2.17428	.19722
				2.17975		2.17461	.19717
10.00000	.51200	.20000	.20000	2.59657	2.47953	2.57229	.18878
				2.60216		2.57667	.18825
10.00000	.72900	.20000	.20000	4.24660	4.00551	4.19609	.18573
				4.25656		4.20386	.18514
11.66700	.72900	.20000	.40000	4.25302	5.52002	4.45765	.25774
				4.26294		4.46637	.25726
100.00000	.51200	.20000	.20000	3.39367	3.09464	3.32933	.17725
				3.41482		3.34559	.17567
100.00000	.72900	.20000	.20000	7.09358	6.14915	6.88218	.16424
				7.15947		6.93169	.16182
100000.00000	.72900	.00000	.20000	6.76900	9.35985	7.45705	.10165
				6.80597		7.48692	.10005
100000.00000	.72900	.20000	.20000	7.67556	6.54732	7.41984	.16002
				7.76497		7.48650	.15697
100000.00000	.72900	.40000	.20000	11.45786	4.51468	10.39236	.26981
				11.94772		10.76603	.26153

Table 3. Polycubic stiffness bounds for plain TROC-composite.

4. Analysis of defective particulate composite

Particulate composites with defective phase contact are considered in a FEM-analysis just as the TROC-material. A thin layer of "voids" (or zones of missing phase contact), however, is spread over the surface of the particle phase covering several fractions of the total surface. The degree of missing phase contact is defined by Equation 6 where S denotes particle surface.

$\chi = S_{\text{inactive}}/S_{\text{total}} \quad \text{degree of missing phase contact}$ $c_a = \chi c [(1 + \Delta)^3 - 1] \quad \text{associated void volume}$	(6)
--	-----

Each zone of missing phase contact may be covered by a void of uniform thickness Δ (relative to mean radius vector of particle) which is related to void concentration c_a (relative to composite volume) and χ as given in Equation 6.

Remark: The zones of missing contact are introduced into FEM-analysis by simple joint-cutting and by finite elements of no stiffness. Sufficient openings are assumed between opposite zone faces such that load does not produce closure effects.

4.1 FEM-setup and results

The FEM models used have an area of missing phase contact centrally placed on each of the 6-edge faces ($N = 8$) or on each of the 4-edge faces ($N = 6$) of the TROC-particle. A number of FEM-experiments have been made varying the stiffness parameters, the volume concentrations (see Figure 5) and degree (α) of missing phase contact. The variables are summarized as follows:

Variables: $c = 0.25, v_S = v_P = 0.2, n = 0.1-10, \chi = 22\%-78\%, c_a = 0-6\%$ $c = 0.42, v_S = v_P = 0.2: n = 1-10 \text{ with } \chi = 42\% \text{ and } c_a = 4.1\%$

The raw data obtained from the axial experiment (σ_X, σ_Y) and the shear experiment (σ_{XY}) are presented in Table 4. Cubic stiffness parameters derived from these data by Equations 2 and 3 are presented in Table 5. Isotropic stiffness parameters derived from Equations 4 and 5 are presented in Table 6.

Defects as cracks

$\chi = 78\%$ corresponds to no contact at all between matrix and 6-edge faces of particle. $\chi = 0.224$ corresponds to no contact at all between matrix and 4-edge faces of particle.

The defective areas including voids correspond to short hollow cylindrical fibres the characteristics of which can be calculated by Equation 7. H is height of composite element, h is corresponding height of inclusion. $N = 8$ for number of 6-edge faces per TROC-particle. $N = 4$ for number of 4-edge faces per TROC-particle.

Fibre diameter: d (diameter of void)

Fibre aspect ratio: $A = l/d$ (l is length of fibre = thickness of void)

Crack density: p (number of cracks per volume unit)

Crack parameter: pd^3 (easily calculated by (4))

$$\begin{aligned}
 d &= h * \sqrt{\frac{3\chi}{8\pi}(1+2\sqrt{3})} \text{ where } h = H * \sqrt[3]{c} \text{ (crack diameter)} \\
 p &= \frac{2Nc}{h^3} \text{ (crack density)} \Rightarrow pd^3 = 2N * c * \left(\frac{3\chi}{8\pi}(1+2\sqrt{3})\right)^{3/2} \\
 A &= \frac{4\chi c}{\pi pd^3} [(1+\Delta)^3 - 1] \text{ (aspect ratio)}
 \end{aligned}
 \tag{7}$$

A cracked homogeneous material

A 'defective particulate composite' with a stiffness ratio of $n = 1$ is of special interest because this composite is, in fact, a cracked homogeneous material. One such material with cracks placed on the 8-edge faces of fictitious TROC-particles is defined in Equation 8. The crack characteristics (pd^3, A) are calculated by Equation 7 with geometrical information introduced from Table 6. The (cracked) materials stiffness associated (E/E_S) is also shown in Equation 8.

$$\begin{aligned}
 (c, N, \chi, \Delta) = (0.25, 8, 0.3128, 0) &\Rightarrow \begin{cases} pd^3 = 0.272 \\ A = 0 \\ E/E_S = 0.96 \end{cases} \\
 (c, N, \chi, \Delta) = (0.25, 8, 0.3128, 0.1111) &\Rightarrow \begin{cases} pd^3 = 0.272 \\ A = 0.136 \\ E/E_S = 0.92 \end{cases} \\
 (c, N, \chi, \Delta) = (0.422, 8, 0.497, 0.067) &\Rightarrow \begin{cases} pd^3 = 0.92 \\ A = 0.0623 \\ E/E_S = 0.82 \end{cases}
 \end{aligned}
 \tag{8}$$

n	c	E _S	χ	N	Δ	c _A	σ _x	σ _z	σ _{xy}
0.1	0.25	3.e5	0.0	8.	0.0	0.0	5.64187	21.4337	16.6075
0.1	0.25	3.e5	0.3128	8.	0.0	0.0	5.52754	21.0901	16.4699
0.1	0.25	3.e5	0.3128	8.	0.1111	0.0252	5.30531	20.3145	15.7044
0.1	0.25	3.e5	0.7760	8.	0.0	0.0	5.31115	20.2065	15.8471
0.1	0.25	3.e5	0.7760	8.	0.1111	0.0596	4.78016	18.0350	13.9938
1.0	0.25	3.e5	0.3128	8.	0.0	0.0	7.63060	31.7567	24.1558
1.0	0.25	3.e5	0.3128	8.	0.1111	0.0252	7.47874	30.5322	23.1879
2.3333	0.25	3.e5	0.2240	6.	0.1111	0.0232	9.07449	37.0004	28.4921
2.3333	0.25	3.e5	0.3128	8.	0.0	0.0	9.13265	38.5681	29.4133
2.3333	0.25	3.e5	0.3128	8.	0.1111	0.0252	8.91010	37.0617	28.1979
2.3333	0.25	3.e5	0.7760	8.	0.0	0.0	6.43111	31.9672	24.7755
2.3333	0.25	3.e5	0.7760	8.	0.0317	0.0170	6.47292	30.8845	23.9469
2.3333	0.25	3.e5	0.7760	8.	0.1111	0.0596	6.47904	29.4582	22.6830
10.	0.25	3.e5	0.0	8.	0.0	0.0	12.9076	50.7740	39.5445
10.	0.25	3.e5	0.3128	8.	0.0	0.0	11.2129	47.9405	37.4999
10.	0.25	3.e5	0.3128	8.	0.1111	0.0252	10.7837	46.0183	35.7760
10.	0.25	3.e5	0.7760	8.	0.0	0.0	6.93955	38.9623	30.7241
10.	0.25	3.e5	0.7760	8.	0.1111	0.0596	7.15779	35.4200	27.2428
1.	0.422	3.e5	0.497	8.	0.067	0.041	6.37132	26.7849	20.6577
10.	0.422	3.e5	0.497	8.	0.067	0.041	11.1205	53.4810	41.3576

Table 4. Reaction stresses (kp/cm^2) in experiments on defective TROC-composite. Axial σ_x and σ_y . Shear: σ_{xy} .

n	c	χ	Δ	c_A	E_{CUB}/E_S	ν_{CUB}	G_{CUB}/G_S
.100000	.25000	.00000	.00000	.00000	.63608	.20837	.66430
.100000	.25000	.31280	.00000	.00000	.62648	.20766	.65880
.100000	.25000	.31280	.11110	.02520	.60391	.20708	.62818
.100000	.25000	.77600	.00000	.00000	.59985	.20814	.63388
.100000	.25000	.77600	.11110	.05960	.53440	.20952	.55975
1.000000	.25000	.31280	.00000	.00000	.96000	.19373	.96623
1.000000	.25000	.31280	.11110	.02520	.91964	.19675	.92752
2.333300	.25000	.22400	.11110	.02320	1.11420	.19695	1.13968
2.333300	.25000	.31280	.00000	.00000	1.16904	.19146	1.17653
2.333300	.25000	.31280	.11110	.02520	1.12026	.19382	1.12792
2.333300	.25000	.77600	.00000	.00000	.99377	.16748	.99102
2.333300	.25000	.77600	.03170	.01700	.95471	.17327	.95788
2.333300	.25000	.77600	.11110	.05960	.90407	.18029	.90732
10.000000	.25000	.00000	.00000	.00000	1.51805	.20269	1.58178
10.000000	.25000	.31280	.00000	.00000	1.45632	.18956	1.50000
10.000000	.25000	.31280	.11110	.02520	1.39746	.18985	1.43104
10.000000	.25000	.77600	.00000	.00000	1.22880	.15118	1.22896
10.000000	.25000	.77600	.11110	.05960	1.10045	.16811	1.08971
1.000000	.42200	.49700	.06700	.04100	.81121	.19216	.82631
10.000000	.42200	.49700	.06700	.04100	1.65508	.17214	1.65430

Table 5. Cubic stiffness of defective TROC-composite.

n	c	χ	Δ	c_A	G/G_S	K/K_S	E/E_S	ν
.100000	.25000	.00000	.00000	.00000	.65085	.65435	.65155	.20128
.100000	.25000	.31280	.00000	.00000	.65125	.65187	.65187	.20114
.100000	.25000	.31280	.11110	.02520	.64378	.64290	.64361	.19967
.100000	.25000	.77600	.00000	.00000	.64428	.64400	.64400	.19949
.100000	.25000	.77600	.11110	.05960	.61675	.61850	.61710	.20068
.100000	.25000	.77600	.03170	.01700	.61705	.61734	.61734	.20056
.100000	.25000	.77600	.11110	.05960	.61809	.61658	.61778	.19941
.100000	.25000	.77600	.11110	.05960	.61866	.61824	.61824	.19919
.100000	.25000	.77600	.11110	.05960	.54754	.55191	.54841	.20190
.100000	.25000	.77600	.11110	.05960	.54793	.54872	.54872	.20173
1.000000	.25000	.31280	.00000	.00000	.96576	.94036	.96057	.19355
1.000000	.25000	.31280	.11110	.02520	.96576	.96057	.96057	.19355
1.000000	.25000	.31280	.11110	.02520	.92536	.90979	.92220	.19591
1.000000	.25000	.31280	.11110	.02520	.92537	.92221	.92221	.19591
2.333300	.25000	.22400	.11110	.02320	1.13052	1.10299	1.12490	.19404
2.333300	.25000	.31280	.00000	.00000	1.13063	1.12499	1.12499	.19402
2.333300	.25000	.31280	.11110	.02520	1.17689	1.13667	1.16862	.19157
2.333300	.25000	.31280	.11110	.02520	1.17689	1.16862	1.16862	.19157
2.333300	.25000	.77600	.00000	.00000	1.12717	1.09764	1.12114	.19358
2.333300	.25000	.77600	.00000	.00000	1.12718	1.12114	1.12114	.19358
2.333300	.25000	.77600	.03170	.01700	1.00297	.89659	.97972	.17218
2.333300	.25000	.77600	.03170	.01700	1.00319	.97989	.97989	.17213
2.333300	.25000	.77600	.11110	.05960	.96523	.87661	.94610	.17622
2.333300	.25000	.77600	.11110	.05960	.96531	.94616	.94616	.17620
2.333300	.25000	.77600	.11110	.05960	.91202	.84833	.89853	.18225
2.333300	.25000	.77600	.11110	.05960	.91206	.89856	.89856	.18224
10.000000	.25000	.00000	.00000	.00000	1.55423	1.53178	1.54969	.19649
10.000000	.25000	.31280	.00000	.00000	1.55493	1.55025	1.55025	.19638
10.000000	.25000	.31280	.11110	.02520	1.48748	1.40733	1.47073	.18648
10.000000	.25000	.31280	.11110	.02520	1.48764	1.47085	1.47085	.18646
10.000000	.25000	.77600	.00000	.00000	1.42230	1.35171	1.40760	.18760
10.000000	.25000	.77600	.00000	.00000	1.42238	1.40766	1.40766	.18758
10.000000	.25000	.77600	.11110	.05960	1.24923	1.05683	1.20534	.15784
10.000000	.25000	.77600	.11110	.05960	1.24974	1.20572	1.20572	.15773
10.000000	.25000	.77600	.11110	.05960	1.10566	.99471	1.08154	.17381
10.000000	.25000	.77600	.11110	.05960	1.10602	1.08181	1.08181	.17373
1.000000	.42200	.49700	.06700	.04100	.82237	.79055	.81581	.19042
1.000000	.42200	.49700	.06700	.04100	.82240	.81583	.81583	.19041
10.000000	.42200	.49700	.06700	.04100	1.67012	1.51444	1.63648	.17583
10.000000	.42200	.49700	.06700	.04100	1.67035	1.63665	1.63665	.17579

Table 6. Poly-cubic stiffness bounds for defective TROC-composite.

5. Pearls on a string composite (CC-CC)

The FEM-analysis of a TROC-material is also used in an analysis of composites where particles have grown together changing phase P from being discrete to being continuous like pearls on a string - or in other words, from being a closed "pore" system to being an open "pore" system.

5.1 FEM-setup and results

FEM-setup is as explained in Figures 1 - 7. The "pearls on a string" geometry of phase P is obtained by interconnecting the TROC-particles between the 6-edge faces of the TROC-particles. Cylindrical tunnels are formed by letting the finite elements between particles, see Figure 5, take the properties of the particles. The volume fraction of phase P TROC-particles relative to total phase P volume (both TROC and tunnels) is denoted by α .

A number of FEM-experiments have been made on Pearls on a string composites defined as follows:

Variables:	$c = 0.36, \alpha = 60\%, v_s = v_p = 0.2: n = 0 - 10$
	$c = 0.45, \alpha = 76\%, v_s = v_p = 0.2: n = 0 \text{ and } 100$
	$c = 0.67, \alpha = 76\%, v_s = v_p = 0.2: n = 0 - 100$

The raw data obtained from the axial experiment (σ_x, σ_y) and the shear experiment (σ_{xy}) are presented in Table 7. Cubic stiffness parameters derived from these data by Equations 2 and 3 are presented in Table D8. Isotropic stiffness parameters derived from Equations 4 and 5 are presented in Table 9.

n	c	$\alpha(\%)$	E_s	v_s	v_p	σ_x	σ_y	σ_{xy}
0.	.36	60.	8.e5	.2	.2	8.34233	36.98560	24.36056
.333333	.36	60.	2.e5	.2	.2	3.78127	15.24916	11.37820
3.	.36	60.	2.e5	.2	.2	8.49105	32.80770	25.30464
10.	.36	60.	2.e5	.2	.2	16.42488	51.60347	45.69911
1.e-5	.451	76.	2.e5	.2	.2	1.729845	7.21862	4.77155
100.	.451	76.	2.e5	.2	.2	124.22087	286.63932	321.55018
1.e-5	.674	76.	2.e5	.2	.2	0.65792	3.43617	1.46436
.333333	.674	76.	2.e5	.2	.2	2.66456	10.89348	7.99115
3.	.674	76.	2.e5	.2	.2	11.67492	46.63378	35.29817
10.	.674	76.	2.e5	.2	.2	28.42779	107.75521	86.38002
100.	.674	76.	2.e5	.2	.2	229.42133	770.07510	679.22262

Table 7. Reaction stresses (kp/cm^2) in experiments on Pearls on a String TROC-composite. Axial σ_x and σ_y . Shear: σ_{xy} .

n	c	$\alpha(\%)$	v_s	v_p	E_{CUB}/E_s	v_{CUB}	G_{CUB}/G_s
.00000	.36000	60.	.20000	.20000	.42394	.18404	.36541
.33333	.36000	60.	.20000	.20000	.68733	.19870	.68269
3.00000	.36000	60.	.20000	.20000	1.46581	.20560	1.51828
10.00000	.36000	60.	.20000	.20000	2.18361	.24144	2.74195
.00001	.45100	76.	.20000	.20000	.32749	.19331	.28629
100.00000	.45100	76.	.20000	.20000	10.57623	.30234	19.29301
.00001	.67400	76.	.20000	.20000	.16124	.16070	.08786
.33333	.67400	76.	.20000	.20000	.49231	.19653	.47947
3.00000	.67400	76.	.20000	.20000	2.09793	.20023	2.11789
10.00000	.67400	76.	.20000	.20000	4.79434	.20875	5.18280
100.00000	.67400	76.	.20000	.20000	33.23769	.22954	40.75335

Table 8. Cubic stiffness of Pearls on a String TROC-composite.

FEM analysis of two basic composites

n	c($\alpha\%$)	v_s	v_p	G/G_s	K/K_s	E/E_s	ν
.00000	.360(60)	.20000	.20000		.38865	.40253	.39135
					.39110		.20685
.33333	.360(60)	.20000	.20000		.68483	.68435	.68474
					.68484		.19983
3.00000	.360(60)	.20000	.20000		1.49400	1.49369	1.49394
					1.49457		.19995
10.00000	.360(60)	.20000	.20000		2.44899	2.53360	1.49439
					2.48945		.19986
							2.0807
							2.49816
							.20420
.00001	.451(76)	.20000	.20000		.30208	.32035	.30557
					.30351		.21384
100.00000	.451(76)	.20000	.20000		13.86086	16.05243	.30673
					15.47385		.21275
							14.24996
							23369
							15.58620
							.20871
.00001	.674(76)	.20000	.20000		.10836	.14256	.11382
					.11939		.26048
.33333	.674(76)	.20000	.20000		.48508	.48668	.12341
					.48518		.24031
3.00000	.674(76)	.20000	.20000		2.10970	2.09951	.48540
					2.10975		.20079
10.00000	.674(76)	.20000	.20000		5.00482	4.93832	.48548
					5.01354		.20074
							2.10765
							.19884
							2.10769
							.19883
							4.99138
							.19678
							4.99831
							.19636
100.00000	.674(76)	.20000	.20000		36.96384	36.86753	36.94454
					37.42770		.19937
							37.31431
							.19636

Table 9. Poly-cubic stiffness bounds for Pearls on a String TROC-composite.

6. Grid composite (CC-CC)

6.1 Model

The so-called CROSS-composite shown in Figure 8 is considered. It is a phase symmetric cubic frame work of phase P embedded in a complementary cubic frame work of phase S. The composite element and the basic cell of a CROSS-composite are shown in Figure 9.

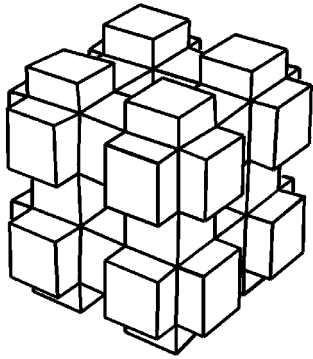


Figure 8. CROSS-composite

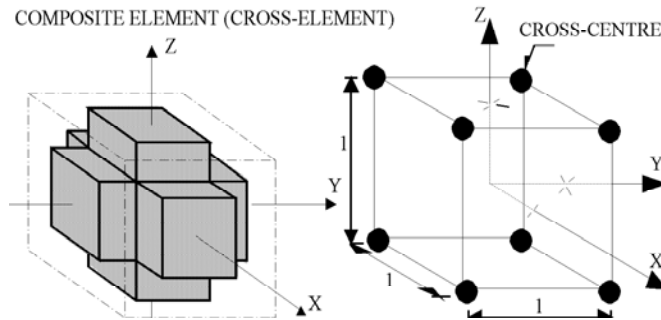


Figure 9. Composite element and basic cell for CROSS-composite. Both heights are 1.

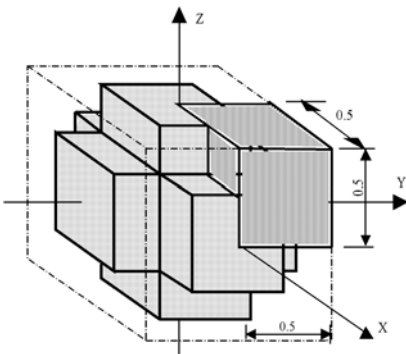


Figure 10. Shaded box is test volume for FEM-analysis. Length unit 1 is height of composite element.

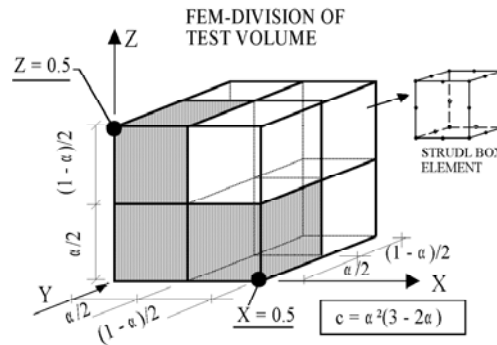


Figure 11. FEM-structure of test volume. Size of FEM-elements and phase P concentration (c) is regulated by $0 \leq \alpha \leq 1$ as indicated.

6.2 Test volume and FEM-division

Due to symmetry and antimetry with respect to both materials model and the FEM-setup, subsequently explained, a test volume of only 1/64 of the basic cell is used in the stiffness analysis of CROSS-composites. The composite element, basic cell and test volume are shown in Figures 9 and 10.

The very simple FEM-structure of the test volume shown in Figure 11 is made possible combining the cubic regularity of the composite element with very refined STRUDL box type elements, see Figure 11, defined in (11). It is indicated in Figure 11 how volume concentrations (c) can be chosen arbitrarily in analysis.

The supporting joints in planes $X = 1/2$ and $Z = 1/2$ are modified by infinitely stiff bars to pick up reaction forces on the test volume. The version of the finite element program applied, STRUDL (11), is unable to give reactions directly from finite element joints.

AXIAL EXPERIMENT

Conditions: All joints in faces of test volume are smoothly supported against infinitely stiff parallel walls.

Load: Joints in face $Z = 0$ are moved $0.5 \cdot 10^{-4}$ in Z-direction.

Response: Sum of Z-forces picked up from bars in face $Z = 1/2$.

SHEAR EXPERIMENT

Conditions: All joints in planes $Z = 0$ and $Z = 1/2$ are smoothly supported against infinitely stiff parallel walls. The joints in planes $Y = 0$ and $Y = 1/2$ can move freely only in Y-direction. Joints in $X = 0$ and $X = 1/2$ can move freely only in X-direction.

Load: All joints in plane $Y = 0$ are moved $0.5 \cdot 10^{-4}$ in X-direction. All joints in $X = 0$ are moved $0.5 \cdot 10^{-4}$ in Y-direction

Response: Sum of Y-forces picked up from bars in plane $X = 1/2$

CONTROL EXPERIMENT (spot checks only)

Conditions: As in axial experiment.

Load: Joints in plane $Z = 0$ are moved $0.5 \cdot 10^{-4}$ in Z-direction. Joints in plane $X = 0$ are moved $0.5 \cdot 10^{-4}$ in X-direction. Joints in plane $Y = 0$ are moved $0.5 \cdot 10^{-4}$ in Y-direction.

Response: Sum of Z-forces picked up from bars in plane $Z = 1/2$ (= sum of X-forces picked up from bars in plane $X = 1/2$).

FEM-setup

The following set-ups are designed to execute the experiments outlined in Equations 1-3. The average strain is joint movement divided by associated length (0.5) of test volume, see Figure 10. The average stress is sum of bar forces divided by associated surface area (0.25) of test volume, see Figure 10 again.

FEM-results

A number of FEM-experiments have been made varying the stiffness parameters and the volume concentrations, c , of the CROSS-model. The variables are summarized as follows:

Variables: $c = 0.25 - 0.75$, $\nu_p = \nu_s = 0.2$, $n = 0 - 10^3$

The raw data obtained from the axial experiment (σ_X, σ_Y) and the shear experiment (σ_{XY}) are presented in Table 10. Cubic stiffness parameters derived from these data by Equations 2 and 3 are presented in Table 11. Isotropic stiffness parameters derived from Equations 4 and 5 are presented in Table 12.

FEM analysis of two basic composites

n	c	E _s	v _s	v _p	σ _x	σ _y	σ _{xy}
5.e-6	.2522	2.e5	.2	.2	2.34360	12.2310	7.56482
.01	.2522	2.e5	.2	.2	2.42376	12.4551	7.79996
.1	.2522	2.e5	.2	.2	3.04553	14.1795	9.56759
.333333	.2522	2.e5	.2	.2	4.11096	17.2564	12.5175
3.	.2522	2.e5	.2	.2	7.10379	30.3116	21.5464
10.	.2522	2.e5	.2	.2	9.18508	49.9761	27.8779
100.	.2522	2.e5	.2	.2	27.1192	275.502	67.9144
1000.	.2522	2.e5	.2	.2	203.517	2515.67	443.012
0.	.5	2.e5	.2	.2	.830440	6.23841	2.45587
.001	.5	2.e5	.2	.2	.839332	6.26705	2.48726
.01	.5	2.e5	.2	.2	.918772	6.52110	2.76339
.1	.5	2.e5	.2	.2	1.64688	8.78233	5.11944
.333333	.5	2.e5	.2	.2	3.08359	13.3206	9.39984
1.	.5	2.e5	.2	.2	5.55480	22.2220	16.6656
10.	.5	2.e5	.2	.2	16.4687	87.8232	51.1945
0.	.7478	2.e5	.2	.2	.195981	2.48889	.416377
.01	.7478	2.e5	.2	.2	.271191	2.75504	.679140
.1	.7478	2.e5	.2	.2	.918508	4.99762	2.78779
1000.	.7478	2.e5	.2	.2	2351.29	12252.7	7588.46

Table 10. Reaction stresses (kp/cm²) in experiments on CROSS-composite. Axial σ_x and σ_y. Shear: σ_{xy}.

n	c	v _s	v _p	E _{CUB} /E _s	v _{CUB}	G _{CUB} /G _s
5.e-6	.25220	.20000	.20000	.57386	.16080	.45389
.01000	.25220	.20000	.20000	.58327	.16290	.46800
.10000	.25220	.20000	.20000	.65513	.17681	.57406
.33333	.25220	.20000	.20000	.78373	.19239	.75105
3.00000	.25220	.20000	.20000	1.38071	.18986	1.29278
10.00000	.25220	.20000	.20000	2.35620	.15526	1.67267
100.00000	.25220	.20000	.20000	13.53207	.08961	4.07486
1000.00000	.25220	.20000	.20000	124.26030	.07484	26.58072
.00000	.50000	.20000	.20000	.30216	.11748	.14735
.00100	.50000	.20000	.20000	.30344	.11811	.14924
.01000	.50000	.20000	.20000	.31471	.12349	.16580
.10000	.50000	.20000	.20000	.41311	.15791	.30717
.33333	.50000	.20000	.20000	.60807	.18798	.56399
1.00000	.50000	.20000	.20000	1.00002	.19997	.99994
10.00000	.50000	.20000	.20000	4.13110	.15791	3.07167
.00000	.74780	.20000	.20000	.12301	.07299	.02498
.01000	.74780	.20000	.20000	.13532	.08961	.04075
.10000	.74780	.20000	.20000	.23562	.15525	.16727
1000.00000	.74780	.20000	.20000	574.77850	.16100	455.30760

Table 11. Cubic stiffness of CROSS-composite.

FEM analysis of two basic composites

n	c	v_s	v_p	G/G_s	K/K_s	E/E_s	v
5.e-6	.25220	.20000	.20000	.50096	.50755	.50226	.20312
				.50963	-	.50921	.19901
.01000	.25220	.20000	.20000	.51371	.51908	.51477	.20249
				.52155	-	.52105	.19886
.10000	.25220	.20000	.20000	.60829	.60812	.60825	.19993
				.61165	-	.61094	.19861
.33333	.25220	.20000	.20000	.76568	.76435	.76541	.19958
				.76612	-	.76577	.19944
3.00000	.25220	.20000	.20000	1.33089	1.33558	1.33183	.20084
				1.33266	-	1.33324	.20052
10.00000	.25220	.20000	.20000	1.91519	2.05039	1.94078	.21604
				1.98256	-	1.99579	.20799
100.00000	.25220	.20000	.20000	5.74434	9.89221	6.27016	.30985
				8.40611	-	8.66650	.23717
1000.00000	.25220	.20000	.20000	39.28336	87.68112	44.15820	.34891
				71.44010	-	74.18846	.24616
.00000	.50000	.20000	.20000	.18851	.23698	.19655	.25117
				.21820	-	.22172	.21932
.00100	.50000	.20000	.20000	.19052	.23837	.19849	.25019
				.21981	-	.22328	.21899
.01000	.50000	.20000	.20000	.20796	.25076	.21531	.24242
				.23394	-	.23712	.21632
.10000	.50000	.20000	.20000	.34630	.36228	.34939	.21068
				.35555	-	.35688	.20448
.33333	.50000	.20000	.20000	.58306	.58463	.58338	.20064
				.58408	-	.58419	.20023
1.00000	.50000	.20000	.20000	.99998	.99992	1.00002	.19999
				.99998	-	1.00002	.19999
10.00000	.50000	.20000	.20000	3.46304	3.62282	3.49386	.21068
				3.55551	-	3.56877	.20448
.00000	.74780	.20000	.20000	.03714	.08643	.04192	.35448
				.07002	-	.07278	.24736
.01000	.74780	.20000	.20000	.05744	.09892	.06270	.30985
				.08406	-	.08667	.23717
.10000	.74780	.20000	.20000	.19152	.20504	.19408	.21604
				.19826	-	.19958	.20799
1000.00000	.74780	.20000	.20000	502.23610	508.65840	503.50760	.20304
				510.81840	-	510.38490	.19898

Table 12. Poly-cubic stiffness bounds for CROSS-composite.

7. On the accuracy of FEM-analysis

Approximately every second cubic bulk $K_C = E_C/(1 - 2\nu_C)$ obtained from axial experiments are checked by the control experiment explained in Equation 3. The results agree within the first five significant digits. The isotropic Young's modulus for $n = 1$ and $\nu_P = \nu_S = 0.2$ is calculated with an accuracy < 1 o/oo. It is concluded from these observations that the FEM-partitioning used in the analysis is appropriate in general, and that numerical errors are very modest at moderate stiffness ratios.

In general no accurate error analysis can be made on the stiffness moduli predicted by FEM-analysis. Some valuable estimates on accuracy, however, can be made at $\nu_P = \nu_S = 0.2$ from Equation 9 which is an adapted compilation of expressions presented in appropriate theoretical expressions in (1,2).

$$\theta_{FEM} = \frac{[n - c(n-1)]e_{FEM} - n}{1 + c(n-1) - e_{FEM}} \quad \left(\begin{array}{l} n < \theta_{FEM} < 1 \text{ at } n < 1 \\ 1 < \theta_{FEM} < n \text{ at } n > 1 \end{array} \right)$$

$$e_{FEM}(n, c) = \frac{1}{e_{FEM}(1/n, c)} \quad (\text{CSA}_P) \quad (9)$$

$$e_{FEM}(n, c) = n * e_{FEM}(1/n, 1 - c) \quad (\text{Phase-symmetry})$$

- The former expression checks that no FEM results violate the H/S bounds. A high accuracy of the FEM-analysis is indicated by a continuous and smooth development of $\theta_{FEM}(c)$ at increasing stiffness ratios, n . Particulate composites will have $\theta_{FEM}(c)$ close to 1. Phase-symmetric composites will have $\theta_{FEM}(c)$ closer to n .
- The second expression can be used to check the accuracy of the FEM-analysis of the TROC material assuming that this material behaves as a CSP_P composite
- The latter expression can be used to check the FEM-analysis of the CROSS material because this material is in fact phase-symmetric.

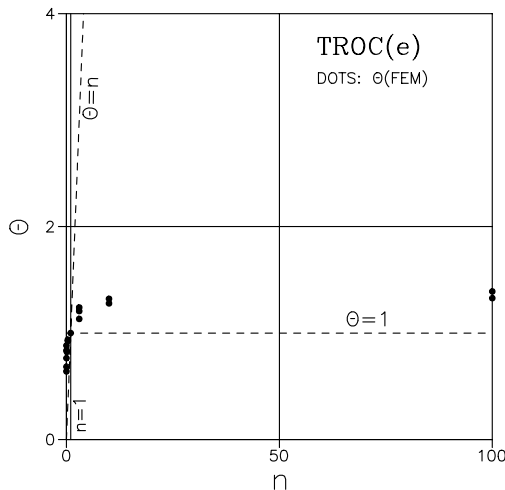


Figure 12. TROC-composite with $\nu_P = \nu_S = 0.2$: θ -test on FEM-data obtained to determine Young's modulus.

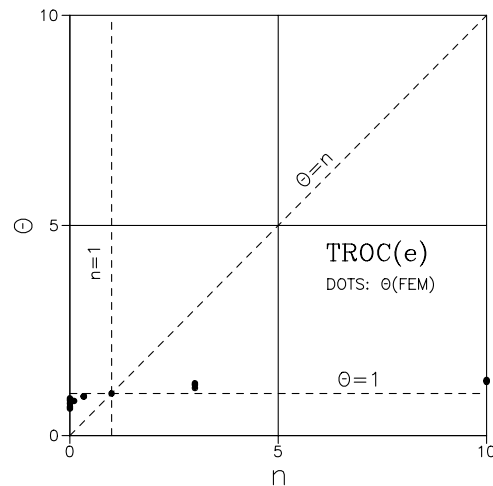


Figure 13. TROC-composite with $\nu_P = \nu_S = 0.2$: θ -test on FEM-data obtained to determine Young's modulus.

The TROC FEM-results (with $\nu_p = \nu_s = 0.2$) have been checked by the former expression in Equation 9. No violations of the H/S bounds were found (Figures 12 and 13). It was observed that $\theta_{FEM}(c)$ keeps very much to ≈ 1 , meaning that the material tested behaves approximately as a CSA_P composite (Figure 14). An accuracy of about 1% is then calculated by the second expression in Equation 9.

Also for the CROSS FEM-results (with $\nu_p = \nu_s = 0.2$), no violations of the H/S bounds were found (Figures 15 and 16). The phase-symmetric geometry is confirmed which means that an accuracy of $\ll 1\%$ is calculated by the latter term in Equation 9.

Conclusion: From the above discussion is stated that only very modest errors are attached to the stiffness properties determined by FEM-analysis.

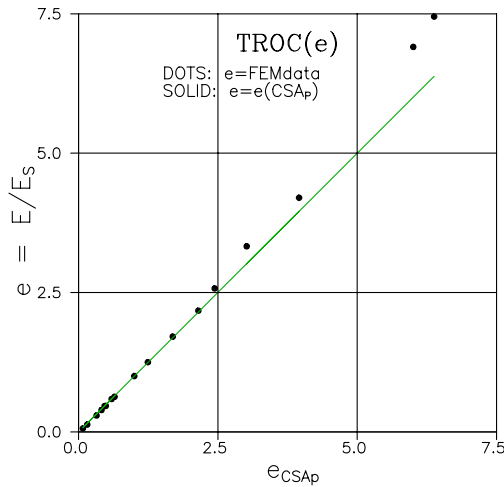


Figure 14. TROC-composite with $\nu_p = \nu_s = 0.2$: FEM-Young's modulus compared with Young's modulus of CSA_P composite.

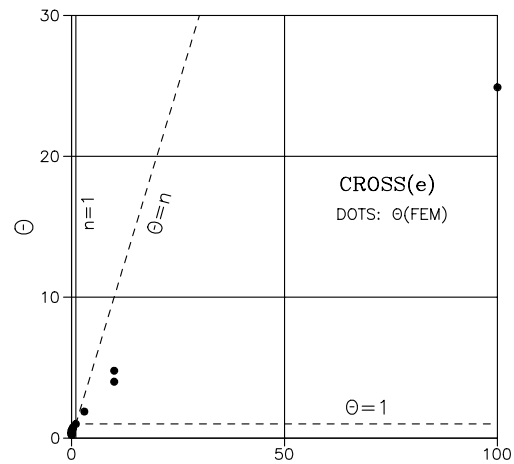


Figure 15. CROSS-composite with $\nu_p = \nu_s = 0.2$: θ -test on FEM-data obtained to determine Young's modulus.

7.1 False data

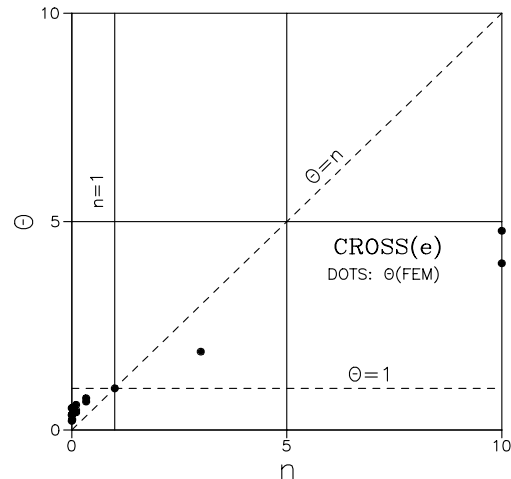


Figure 16. CROSS-composite with $\nu_p = \nu_s = 0.2$: θ -test on FEM-data obtained to determine Young's modulus.

The following rule has been used to exclude false data (mistakes in tests or data treatment): If a description can be made which fits very well a large number of familiar data with only a few data as clear exceptions - then these data can be considered false. Only one false data set was found in this FEM-analysis, namely shear modulus g of the TROC-composite at $(n, \nu_s, \nu_p, c) = (10^5, 0.4, 0.2, 0.73)$. The reason for exclusion is obvious from appropriate Figures in the theoretical works (1,2).

Appendix A - Elasticity

A.1 Isotropy

Stiffness of an isotropic elastic material is defined by the bulk modulus K and the shear modulus G . Young's modulus E , and the Poisson's ratio (ν) together with two ν -parameters (κ and γ) are related to K and G as follows.

$$\begin{aligned} E &= \frac{9KG}{3K+G} \quad ; \quad \nu = \frac{3K-2G}{2(3K+G)} \\ G &= \frac{E}{2(1+\nu)} \quad ; \quad K = \frac{E}{3(1-2\nu)} \\ \kappa &= \frac{2(1-2\nu)}{1+\nu} \quad ; \quad \gamma = \frac{7-5\nu}{2(4-5\nu)} \end{aligned} \quad (A1)$$

A.1.1 Composite aspects

In composite theory it is very often appropriate to relate composite elastic moduli (K , G , E , ν) to elastic moduli (K_S , G_S , E_S , ν_S) of an isotropic reference material S . Dimensionless versions of E and ν are then presented as follows with $k = K/K_S$, $g = G/G_S$, and $e = E/E_S$

$$e = \frac{3kg}{2(1+\nu_S)k + (1-2\nu_S)g} \quad ; \quad \nu = \frac{(1+\nu_S)k - (1-2\nu_S)g}{2(1+\nu_S)k + (1-2\nu_S)g} \quad (A2)$$

A.1.2 Stress-strain

The stress tensor σ_{ij} and the strain tensor ε_{ij} are related as follows (ex 12) when an isotropic elastic material is considered with stiffness properties from Equation A1.

$$\begin{aligned} \varepsilon_{ij} &= \frac{1+\nu}{E} \left(\sigma_{ij} - \delta_{ij} \frac{\nu}{1+\nu} \sigma_{kk} \right) \\ \sigma_{ij} &= \frac{E}{1+\nu} \left(\varepsilon_{ij} + \delta_{ij} \frac{\nu}{1-2\nu} \varepsilon_{kk} \right) \end{aligned} \quad i, j = 1, 2, 3 \quad (A3)$$

with Kroneckers delta $\delta_{ij} = \begin{cases} 1 & \text{if } i = j \\ 0 & \text{if } i \neq j \end{cases}$

Volumetric stress and strain are denoted by $\sigma_{kk} = \sigma_{11} + \sigma_{22} + \sigma_{33}$ and $\varepsilon_{kk} = \varepsilon_{11} + \varepsilon_{22} + \varepsilon_{33}$ respectively. The stress strain relation can also be written as follows in two expressions - one relating volumetric strain to volumetric stress - and another one relating deviatoric strain (e_{ij}) to deviatoric stress (s_{ij}).

$$\begin{aligned} \varepsilon_{kk} &= \frac{\sigma_{kk}}{3K} \quad \text{with} \quad \begin{cases} \varepsilon_{kk} = \varepsilon_{11} + \varepsilon_{22} + \varepsilon_{33} & \text{volumetric strain} \\ \sigma_{kk} = \sigma_{11} + \sigma_{22} + \sigma_{33} & \text{volumetric stress} \end{cases} \\ e_{ij} &= \frac{s_{ij}}{2G} \quad \text{with} \quad \begin{cases} e_{ij} = \varepsilon_{ij} - \delta_{ij} \varepsilon_{kk}/3 & \text{deviatoric strain} \\ s_{ij} = \sigma_{ij} - \delta_{ij} \sigma_{kk}/3 & \text{deviatoric stress} \end{cases} \end{aligned} \quad (A4)$$

A.2 Cubic elasticity

Stiffness of a cubic elastic material is defined by the cubic bulk modulus K_C , the cubic shear modulus G_C , and the cubic Young's modulus E_C or the cubic Poisson's ratio ν_C . The constitutive equation of a cubical elastic material can be expressed as shown in Equation A5 using the coordinate system defined in Figure A1 with stress-strain planes coinciding with planes of elastic symmetry (and materials symmetry).

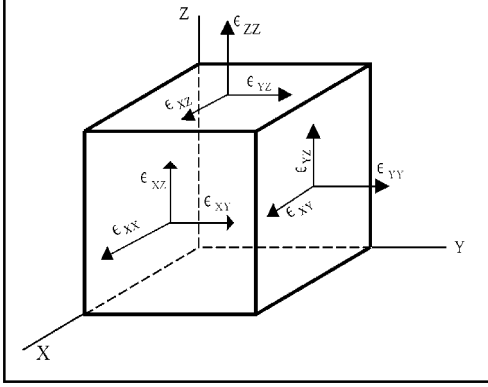


Figure A1. Coordinate system used in FEM-analysis.

Cubic material models are considered in the main text of this report. The stiffness parameters for these materials can be determined performing the two 'FEM-experiments' outlined in Equations A6 and A7. The cubic Young's modulus, the cubic Poisson's ratio, and the cubic bulk modulus are obtained from the "axial experiment" explained in Equation A6. The cubic shear modulus is obtained from the "shear experiment" explained in Equation A7.

$$\begin{bmatrix} \varepsilon_x \\ \varepsilon_y \\ \varepsilon_z \\ \varepsilon_{xy} \\ \varepsilon_{xz} \\ \varepsilon_{yz} \end{bmatrix} = \begin{bmatrix} 1/E_C & -\nu_C/E_C & -\nu_C/E_C & 0 & 0 & 0 \\ -\nu_C/E_C & 1/E_C & -\nu_C/E_C & 0 & 0 & 0 \\ -\nu_C/E_C & -\nu_C/E_C & 1/E_C & 0 & 0 & 0 \\ 0 & 0 & 0 & 1/2G_C & 0 & 0 \\ 0 & 0 & 0 & 0 & 1/2G_C & 0 \\ 0 & 0 & 0 & 0 & 0 & 1/2G_C \end{bmatrix} * \begin{bmatrix} \sigma_x \\ \sigma_y \\ \sigma_z \\ \sigma_{xy} \\ \sigma_{xz} \\ \sigma_{yz} \end{bmatrix} \quad (\text{A5})$$

$$\text{Conditions:} \quad \varepsilon_x = \varepsilon_y = \varepsilon_{xy} = \varepsilon_{xz} = \varepsilon_{yz} = 0$$

$$\text{Load} \Rightarrow \text{response:} \quad \varepsilon_z \Rightarrow \sigma_x (= \sigma_y)$$

$$\text{Results:} \quad E_C = \frac{\sigma_z^2 - 2\sigma_x^2 + \sigma_x\sigma_z}{\varepsilon_z(\sigma_x + \sigma_z)} ; \quad \nu_C = \frac{\sigma_x}{\sigma_x + \sigma_z} \Rightarrow \quad (\text{A6})$$

$$K_C = \frac{E_C}{3(1 - 2\nu_C)}$$

$$\text{Conditions:} \quad \varepsilon_x = \varepsilon_y = \varepsilon_z = \varepsilon_{xz} = \varepsilon_{yz} = 0$$

$$\text{Load} \Rightarrow \text{response:} \quad \varepsilon_{xy} \Rightarrow \sigma_{xy} \quad (\text{A7})$$

$$\text{Result:} \quad G_C = \frac{\sigma_{xy}}{2\varepsilon_{xy}}$$

A.2.1 Poly-cubic elasticity

Isotropic mixtures of parts from a cubic material behave elastically, just as an isotropic mixture of cubic crystals. Equation A8 expresses the exact bulk modulus for such mixtures (13).

$$K = K_C = \frac{E_C}{3(1-2\nu_C)} \quad (A8)$$

No corresponding exact poly-cubic shear modulus solution has yet been found. However, it has been shown (14) that the true value is bounded between two solutions derived in (15,16). Some re-writing of these boundary values imply

$$\left[\frac{1}{G_C} + \frac{2}{5} \left(\frac{2(1+\nu_C)}{E_C} - \frac{1}{G_C} \right) \right]^{-1} \leq G \leq G_C + \frac{2}{5} \left(\frac{E_C}{2(1+\nu_C)} - G_C \right) \quad (A9)$$

The lower bound (16) is based on an assumption which is tantamount to assuming that the state of stress is identical from crystal to crystal. Correspondingly the upper bound (15) assumes identical states of strain. If the crystals were isotropic then Equation A9 predicts $G = G_C$. Improved bounds for poly-crystals have been given by Hashin and Shtrikman (17). For the present work, however, the bounds in Equation A9 suffice. The upper and lower bounds are sufficiently close to justify simple mean value approximations.

A.2.2 Composite aspects

When isotropic mixtures of cubic composite elements are considered it is very often appropriate to relate composite cubic elastic moduli (K_C, G_C, E_C, ν_C) to the elastic moduli (K_S, G_S, E_S, ν_S) of an isotropic reference material S. Normalized versions of Equations A8 and A9 with respect to phase S are presented as follows with relative coefficients of cubical elasticity $k_C = K_C/K_S, g_C = G_C/G_S$, and $e_C = E_C/E_S$,

$$k = k_C = e_C \frac{1-2\nu_S}{1-2\nu_C} \quad \Rightarrow \quad \nu_C = \frac{1}{2} \left(1 - \frac{e_C}{k_C} (1-2\nu_S) \right) \quad (A10)$$

$$\left[\frac{1}{g_C} + \frac{2}{5} \left(\frac{1+\nu_C}{1+\nu_S} \frac{1}{e_C} - \frac{1}{g_C} \right) \right]^{-1} \leq g \leq g_C + \frac{2}{5} \left(\frac{1+\nu_S}{1+\nu_C} e_C - g_C \right)$$

which can also be expressed as follows with ν_C introduced

$$\frac{1}{g} \leq \frac{3}{5g_C} + \frac{1}{5(1+\nu_S)} \left(\frac{3}{e_C} - \frac{1-2\nu_S}{k_C} \right) \quad (A11)$$

$$g \leq \frac{3g_C}{5} + \frac{4(1+\nu_S)}{5} \left(\frac{3}{e_C} - \frac{1-2\nu_S}{k_C} \right)^{-1}$$

Literature

1. Nielsen, L. Fuglsang: "Elastic Properties of Two-Phase Materials", *Materials Science and Engineering*, 52(1982), 39-62.
2. *Idem*: 'Composite Materials - properties as influenced by geometry', Springer Verlag, Berlin, 2005, in Press.
3. *Idem*: "On the Effect of Defective Phase Contact on the Mechanical Behavior of Particulate Composites like Concrete", *Cement and Concrete Research*, 12(1982), 685.
4. *Idem*: "The TROC-material - definition and topology", *Build. Mat. Lab., Tech. Univ. Denmark*, Tech. rep. 32(1974), 31 pp., (Application report on StvF-project 516-3571.B370).
5. *Idem*: "Partikel-armerede materialers elastiske egenskaber". Progress report 1975(feb) on StvF-project 516-3571.B370, 24 sider.
6. *Idem*: "Partikel-armerede materialers elastiske egenskaber I: Perfekt fasekontakt", *Build. Mat. Lab., tech. rep.* 41(1976), 25 sider. (Progress report on StvF-projects 516-3571.B-370 and 516-3748.B-415).
7. *Idem*: "Partikel-armerede materialers elastiske egenskaber II: Defekt fasekontakt", *Build. Mat. Lab., Tech. Univ. Denmark*, tech. rep. 46(1976), 16 pp., (Progress report on StvF-projects 516-3571.B-370 og 516-3748.B-415).
8. *Idem*: "Fase-symmetriske tokomponentmaterialer". Application report mar(1976), 7 pp, StvF 516-6572.B-508.
9. *Idem*: "Elastic properties of isotropic particle-reinforced and phase-symmetric materials". *Build. Mat. Lab., Tech. Univ. Denmark*, tech. rep. 54(1977), 37 pp, (Progress report on StvF-project 516-6572.B-508).
10. *Idem*: "FEM-resultater for nogle kompositmaterialer". *Build. Mat. Lab., Tecg. Univ. Denmark*, Documentation report sep(1981), 14 pp.
11. ICES STRUDL-II, "The structural design language", *Engineering user's manuals*, 1(1968), 1st ed., and 2(1971), 2nd ed., Dept. Civ. Eng., Massachusetts Institute of Technology.
12. Sokolnikoff, J.S.: "Mathematical theory of elasticity", McGraw-Hill, New York, 2nd edn., 1956.
13. Nowick, A.S., and Berry, B.S.: "Anelastic relaxation in crystalline solids", Academic Press, New York, 1972.
14. Hill, R.: "Elastic behaviour of crystalline aggregate", *Proc. Phys. Soc. (London)*, A65(1952), nr 389, 349.
15. Voigt, W.: "Lehrbuch der Krystallphysik", Teubner, Leipzig, 1910 (reprinted, Teubner, Stuttgart, 1966).
16. Reuss, A.: "Berechnung der fliessgrenze von Mischkristallen auf Grund der Plastizitätsbedingung für Einkristalle", *Ztschr. f. angew. Math. u. Mech.*, 9(1929), 49.
17. Hashin, Z. and Shtrikman, S.: "A variational approach to the theory of the elastic behavior of polycrystals", *Mech. Phys. Solids*, 10(1962), 343.